(NASA-CR-161159) BUBBLE BEHAVIOR DURING SOLIDIFICATION IN LOW-GRAVITY Final Report (Grumman Aerospace Corp.) 26 p HC A03/MF A01 CSCL 20D
N79-17881
Unclas
G3/12 14376

BUBBLE BEHAVIOR DURING SOLIDIFICATION IN LOW-GRAVITY

by

John M. Papazian
Research Department
Grumman Aerospace Corporation
Bethpage, New York 11714

and

William R. Wilcox
Clarkson College of Technology
Potsdam, New York

RM-680

Final Report Prepared Under Contract NAS 8-31529

for

Marshall Space Flight Center
Alabama 35812

February 1979

RECEIVED
NASA STI FACILITY
ACCESS DEPT.

NATIONAL AERONAUTICS AND SPACE ADMINISTRATION

Grumman Research Department Memorandum RM-680

BUBBLE BEHAVIOR DURING SOLIDIFICATION IN LOW GRAVITY

Final Report Prepared Under Contract NAS 8-31529

for

Marshall Space Flight Center
National Aeronautics and Space Administration
Alabama 35812

by

John M. Papazian
Research Department
Grumman Aerospace Corporation
Bethpage, New York 11714

and

William R. Wilcox
Clarkson College of Technology
Potsdam, New York

February 1979

Approved by Richard A. Scheuing
Richard A. Scheuing
Director of Research

ACKNOWLEDGEMENTS

The authors wish to thank M. Kesselman for extensive experimental assistance and Prof. M. Glicksman for stimulating technical discussions and for provision of ultra-high purity succinonitrile.

ABSTRACT

This report is a summary of the work done on NASA contract NAS 8-31529. During this project the trapping and behavior of gas bubbles were studied during low-gravity solidification of carbon tetrabromide, a transparent, metal-model material. The flight experiments were performed during two NASA-sponsored sounding rocket flights (SPAR I and SPAR III) and involved gradient freeze solidification of gas saturated melts. Gas bubbles were evolved at the solid-liquid interfaces during the low-gravity intervals. No large-scale thermal migration of bubbles, bubble pushing by the solid-liquid interface, or bubble detachment from the interface were observed during the low-gravity experiments. During the SPAR III experiment, a unique bubble motion-fluid flow event occurred in one specimen: a large bubble moved downward and caused some circulation of the melt. The gas bubbles that were trapped by the solid in commercial purity material formed voids that had a cylindrical shape in SPAR III, in contrast to the spherical shape that had been observed in SPAR I. These shapes were not influenced by the gravity level (10^{-4} g_o versus g_o), but were dependent upon the initial temperature gradient. In higher purity material, however, the shape of the voids changed from cylindrical in one-g to spherical in low-g. Several ground based experiments on bubble migration were also performed. The results showed a profound effect of sample purity on bubble behavior and provide an explanation of the low-gravity observations.

TABLE OF CONTENTS

Item	Page
Introduction	1
Experimental Procedure	2
Results	4
Discussion	7
Summary	13
References	15

LIST OF ILLUSTRATIONS

Figure		Page
1	Appearance of the Specimens at 101s after Lift-Off	18
2	Montage Photograph of the Growth of Specimen B during SPAR III	19
3	Montage Photograph of the Growth of Specimen C during SPAR III	20
4	Bubble Diameters as a Function of Time, Specimen B, SPAR III	21

PRECEDING PAGE BLANK NOT FILMED

INTRODUCTION

This memorandum presents the results of an experiment designed to investigate the behavior of bubbles at a solidification interface and in the melt ahead of the interface in a "low-gravity" environment ($g < 10^{-4}\ g_o$, where $g_o = 980\ cm/s^2$). The experiment was performed on a sounding rocket flight in December 1976 as part of the NASA Space Processing Applications Rockets Project (SPAR). Also reported are the results of laboratory experiments that were performed to further characterize the specimen material (CBr_4), and the results of laboratory tests simulating the unique environment of a sounding rocket flight. The results of a prior experiment in this program have been reported previously (Ref. 1).

The impetus for this research stems from the need to develop techniques for bubble management during crystal growth or metallic solidification processes. When these processes are performed terrestrially, the gravity generated buoyancy force causes bubbles to move and can be employed to remove them from the melt. In low-gravity, however, the buoyancy force is significantly reduced. For small bubbles, the terminal velocity is directly proportional to gravitational acceleration, thus at $g = 10^{-4}\ g_o$ bubbles are virtually static (Ref. 2). In addition, low gravity is expected to favor easier bubble nucleation due to the reduced hydrostatic head, decreased free convection, and increased dispersion of foreign particles (Ref. 3). Easier nucleation and reduced mobility should, therefore, be characteristic of bubble behavior during materials processing operations in low-gravity. In fact, several experiments have already observed such effects (Refs. 4-7).

Two potential "low-gravity" bubble management techniques are the pushing of bubbles by solid-liquid interfaces and the motion of bubbles in a temperature gradient. Both of these phenomena were addressed in this experiment. Briefly, terrestrial experiments have shown that small bubbles can be pushed by slowly moving interfaces ($d \approx 0.1mm$, $R \approx 5\mu m/s$) (Ref. 8), and considerable literature exists on the influence of processing variables on the inclusion of bubbles (porosity) during casting or crystal growth (Refs. 9-18). Similarly, thermal migration of bubbles can be demonstrated in the laboratory (Ref. 19), and

previous experiments have shown that an inverse temperature gradient can counterbalance the terrestrial buoyancy force on a bubble (Refs. 20, 21). With the exception of our SPAR I experiments (Ref. 1), no studies of bubble-interface interaction in low-gravity have been performed, and despite several demonstrations of Marangoni flows in low-gravity (Refs. 22, 23), no one has yet shown that bubbles will migrate in a temperature gradient in the absence of gravity. Reasonable doubt exists as to whether thermocapillary forces will cause bubble motion in low-gravity either in pure one-component fluids or in impure systems with surface active species present.

The approach taken in this experiment was an extremely simple one involving gradient freeze solidification of a gas-saturated, transparent, low entropy of fusion material. Solidification in such materials has been found to be a good simulation of solidification in metals (Ref. 24). During solidification, the liquid phase becomes enriched in rejected (gaseous) solute which eventually nucleates as a bubble at or near the solid-liquid interface. The subsequent behavior of the bubbles was observed during the "low-gravity" coasting phase of a sounding rocket flight by sequential photographs.

EXPERIMENTAL PROCEDURE

Apparatus

The same apparatus was employed for this flight as had been used on SPAR I. Details of the design and construction were given previously (Ref. 1). In brief, the apparatus was a self-contained rocket-qualified unit that provided for gradient freeze solidification of four samples contained in 10mm OD x 100mm long pyrex tubes. A stable, linear temperature gradient was allowed to decay during the flight, thereby causing the sample to solidify. The apparatus was slightly modified for this flight in order to increase the starting temperature gradient to 20°C/cm while preserving the same freezing rate (10 to 20μm/s). Progress of the experiment was recorded using a motorized 35mm camera.

Specimen Preparation

Carbon tetrabromide, a transparent, low entropy of fusion compound was again chosen as the specimen material. Despite the disadvantages of CBr_4, the same material was flown again to provide a valid comparison to the SPAR I results. Filling of the sample tubes with CBr_4 was effected in a manner identical to that described earlier (Ref. 1). For this flight, all of the specimens were saturated with nitrogen. Three of the four specimens (A, B and C) were commercial purity (CP) CBr_4, and the other (D) was zone refined (ZR) CBr_4. As an indication of the purification effected by zone refining, the relative optical absorptivity of a 0.76 M solution of CBr_4 in CCl_4 at 417 nm was reduced from 0.064 to 0.009. Bromine is thought to be the impurity responsible for this coloration; its concentration was substantially reduced by zone refining. The other major residual impurity was bromoform. Complete details of the purification procedures and results are given elsewhere (Ref. 25). This material is unusually difficult to purify because it decomposes at its melting point. The rate of decomposition is greatly reduced by shielding the sample from light, but it cannot be completely suppressed.

Experimental Sequence

The intended sequence of operations for this experiment was:

t_o - 45 min	heater on
t_o - 4 min	heater off
t_o	launch
t_o + 100s	camera starts
t_o + 300s	camera stops

During the 45 minute preheat period, a stable temperature gradient of 20°C/cm was established along the sample tubes with the solid-liquid interface in the field of view of the camera. We chose to begin cooling the sample before launch because ground base experiments had shown that several minutes were required for a stable cooling rate to be established after the heaters were shut off.

RESULTS

Initial Observations

The rocket flight was successful and the apparatus functioned perfectly. The telemetered data show that the camera began operating at t_o + 100s and took pictures at a rate of 1.08 frames/s. Figure 1 is the second frame of the flight film (t = 101s). Payload despin occurred at about 65s, and all accelerations were below 10^{-3} g_o at 78s. Between 85 and 338s no accelerations greater than 10^{-4} g_o were present. Preliminary observations showed that numerous small bubbles were present in the liquid portion of specimens A, B and C; some solidification had already taken place; cylindrical voids were being formed in specimen C; and the solid-liquid interface in specimen D was more planar than in the other specimens. Subsequent frames of the film show that the cylindrical voids continued to grow, the small bubbles remained stationary, and towards the end of the flight a large bubble at the top of B moved downward along one side, causing gentle circulation of the melt (as shown by movement of small nearby bubbles). To aid in reconstruction of the dynamics of the flight experiment, a 16mm cine film was made from the 35mm x 226 exposure flight film.

Growth and Morphology of Voids

Figures 2 and 3 are a sequence of photographs of specimens B and C, respectively. They show how solidification proceeded during the low-gravity interval. The figures show that gas bubbles were generated at the solid-liquid interface and were incorporated into the solid in the form of voids. There is no evidence of pushing of bubbles by the interface. The voids in specimens A, B, and C were cylindrical in shape. The growth direction of the voids was upward and sharply inclined toward the center of the specimen. The locus of the inner ends of the voids defines the solid-liquid interface, which appears to have been roughly hemispherical and concave towards the liquid. Bubbles nucleated repeatedly, apparently near the periphery of the sample. Transmission optical micrographs of specimens A, B, and C show that the cylindrical voids have uneven surfaces and usually being at a small (approximately 0.05 to 0.1 mm diameter) faceted, roughly spherical void (Ref. 26). Some small spherical voids were also present that did not give rise to cylindrical

voids. From stereoscopic observation, it can be seen that the voids are totally enclosed by CBr_4. Many of them are situated at a small distance (approximately 0.1 mm) in from the outer (cylindrical) surface of the sample.

The fourth specimen, D, does not show the same inclined cylindrical void morphology. Some large voids with a generally spherical morphology were grown in. They are, however, much less distinct that the spherical voids observed in SPAR I. It is also evident in Fig. 1 that the interface of specimen D was more planar and more distinct that the interface of the other three specimens. Specimens A, B, and C had a more extensive mushy zone than specimen D. This is a consequence of the higher purity of specimen D.

Several voids were also observed in specimens grown during ground base simulation experiments before the flight. These voids were of a cylindrical morphology with the axis of the cylinder parallel to the growth direction (upward). Small spherical voids were occasionally observed during laboratory simulations, but, in general, cylindrical voids predominated. The number of voids present was small. These observations also held true for the ZR material.

During ground base simulation experiments bubbles were periodically nucleated at the solid-liquid interface. They remained there and grew larger until they reached a critical size of approximatley 0.5 to 1 mm, whereupon they detached from the interface, floated upward, and dissolved in the melt or came to rest at the top of the sample tube. Most of the gas which was evolved at the solid-liquid interface escaped in this manner. Thus, the total volume of voids grown into the ground base simulation specimens was far less than that in the flight specimens. This observation was confirmed by X-radiography of the flight and ground base specimens.

Bubble Phenomena

As a consequence of the dendritic nature and concave shape of the solid-liquid interface, it is difficult to resolve details of the bubble-interface interaction. However, from close inspection of the photographs and microscopic observations of the low-g processed specimens, it seems that large scale, long distance ($\approx$ 1 mm) pushing of bubbles did not occur. Evidence for pushing

would have been direct observation of bubble motion at the interface or observation of a band of bubbles at the end of the low-g processed material.

A great number of small bubbles were present in the liquid portion of the specimens. There were approximately 400 small (approximately 0.1 mm diameter) bubbles in specimen A, 75 in specimen B, 300 in specimen C, and none in specimen D at the beginning of filming. Also visible toward the top of the viewing slot was the lower portion of a large (approximately 4 mm diameter) bubble in specimens B and D. Examination of Figs. 2 and 3 shows that most of the bubbles appear to have been stationary throughout the experiment, but increased in size. Close examination using transparent overlays and repeated viewing of the 16 mm film confirms that none of the bubbles in A, C, and D moved. Motion of the order of 0.1 mm would have been detected. Significant bubble motion occurred, however, in specimen B, as can be seen in Fig. 2. The direction of bubble motion in B was complex, and the motions occurred in two stages. During the interval between t_o + 100 and t_o + 160s, the lower edge of the large bubble moved downward by 0.5 mm. The small bubbles in the center of the liquid region also moved downward, but some small bubbles moved upward and others moved sideways. The small bubbles only moved approximately 0.2 mm. Almost no bubble motion occurred between 160 and 260s, but at 260s the lower edge of the large bubble began to move downward again. The small bubbles also moved: Those in the center of the field of view followed a curved trajectory downward and to the right; those at the top, very near to the large bubble, moved upwards. The large bubble moved 1.3 mm, and the small bubbles moved between 0.3 and 1.1 mm. When viewing this motion speeded up by a factor of 24 on the cine film, one has the distinct impression that the small bubbles were swept along in a fluid flow that was driven by the motion of the large bubble.

The diameters of several bubbles in specimen B were measured every tenth frame. Typical results are plotted in Fig. 4, with a least squares straight line fit to the data. In general, the bubble diameters increased linearly with time and doubled in the 200s of observation. Bubble diameters were not measured in specimens A and C, but had the same qualitative behavior. This behavior is in contrast to that of SPAR I in which bubbles were observed to disappear during the first 100s.

DISCUSSION

There are several important aspects of these results. Among them are the greater void density observed in samples solidified in the absence of gravity; the observation that an initial temperature gradient of 20°C/cm did not cause bubbles to detach from the interface or migrate through the liquid; and the fact that significant bubble pushing by the interface did not occur. These results reinforce the similar observations that were made on SPAR I with an initial temperature gradient of 5°C/cm (Ref. 1). In addition, several laboratory simulations and theoretical calculations were made in order to assist in interpreting these data, as described below.

Some question exists about the effect of rocket despin at 65s on the prelaunch temperature gradient in the liquid portion of the sample tubes. Perhaps the abrupt deceleration (3.5 to 0.2 rev/s in 0.5s) caused fluid motion vigorous enough to level the temperature gradient and hence remove the driving force for thermocapillary motion. Circumstantial evidence tends to discount this possibility (as discussed in Ref. 1); however, laboratory simulations were made to measure the extent of the effect. The flight apparatus containing two specimen tubes with six thermistors each in intimate contact with the hot liquid was spun and despun. Results from these tests showed that spin-up caused temperature shifts to occur in the liquid, but that these changes were largely recovered upon despin (Ref. 27). The maximum effect observed was a 25% reduction of the 20°C/cm gradient to about 15°C/cm. As discussed more fully earlier (Ref. 27), one might expect a greater change to occur in an actual rocket flight because despin would take place in the absence of a stabilizing, vertical acceleration (gravity). However, the results of these tests clearly show that despin does not cause turbulent mixing to occur, but, rather, preserves the density stratification. However, the despin does reorient the direction of the stratification (i.e., density/temperature gradient). This is thought to be the reason why the growth interface is concave toward the liquid in the flight experiment, whereas it was found to be flat in ground base simulation. In sum, therefore, the effect of despin is to reduce somewhat and reorient the temperature gradient in the liquid portion of the sample; the initial temperature gradient is not eliminated by despin.

Void Morphology and Density

Gravitational forces did not appear to affect the void morphology in specimens A, B and C from this flight. Cylindrical voids were observed in both laboratory simulations and the flight experiment. Likewise, all of the specimens from SPAR I displayed spherical void morphology whether processed in the laboratory or in a weightless environment. The exception to this observation is specimen D for SPAR III. This zone-refined material produced only one or two vertical cylindrical voids when processed in the laboratory, but spherical voids were grown in during flight. Previous work in this area has related void morphology to freezing rate (Refs. 9, 12, 14, 16, 17) concentration of dissolved gas (Refs. 11-14, 16) external pressure (Ref. 12), and convection (Ref. 18). It is generally held that with all other parameters constant, low freezing rates lead to bubble pushing; intermediate freezing rates give cylindrical voids; and high freezing rates produce spherical voids (Ref. 9). If the rate of gas evolution at the interface depends on the solidification rate, then this simple picture is no longer valid (Ref. 17). The critical velocity for bubble pushing varies from system to system and has not been widely studied, but is thought to be farily low, approximately 5 μm/s for a planar interface (Ref. 8). A comparison of our flight and ground base results shows that the void morphology seems to be more affected by a change in temperature gradient, G, than by a change in growth rate R. i.e., spherical voids observed with $G = 5°C/cm$, $R = 2.5$ to 14 μm/s, cylindrical voids observed at $G = 20°C/cm$, $R = 10$ to 25 μm/s. It seems therefore, that G, the temperature gradient in the liquid, is a potent factor in determining void morphology in CBr_4.

Our results also show that, in general, the gravity level had little effect on void morphology except for the zone refined material processed on SPAR III (specimen D). The major difference between this sample and the others is a narrower mushy zone. The interface is still dendritic since it was not possible to reduce the impurity content below the minimum for constitutional supercooling, but the thickness of the dendritic zone was considerably reduced. One might speculate that a gas bubble confined to an interdendritic channel and forced upward by buoyancy is more likely to develop into a cylindrical rather than spherical void, but our data are too sparse to allow an understanding of the effect.

The greater number of voids observed during low gravity solidification on SPAR I and SPAR III might be simply explained. If the same quantity of gas were evolved and the same number of bubbles nucleated irrespective of gravitational forces, then one expects more voids in the low-g specimens because of the lack of buoyancy forces. The buoyancy forces detach bubbles from the interface and sweep them out of the liquid. However, the absence of gravity can also lead to an enhanced nucleation rate because of the reduced hydrostatic head (Ref. 9). This effect may be significant in heterogenous nucleation and is routinely exploited in molten metal degassing operations (Ref. 10). An enhanced nucleation rate could explain the extremely large number of voids observed in A, B, and C of SPAR III. In particular, Fig. 3 shows that many voids originated at bubbles which were nucleated shortly after solidification began. Measurements of void length and knowledge of the growth rate show that the voids first appeared at t_o + 70s, which coincides with establishment of low gravity. Also, it was observed that the voids in the low-gravity specimens were nucleated repeatedly and at many locations along the interface, whereas in one-g a far smaller total number of gas bubbles are nucleated. Further, the large number of bubbles in the liquid portion may also be evidence of enhanced nulceation in low-gravity as mentioned below.

Bubble Growth and Motion

The fortuitous presence of so many small bubbles in the liquid portions of A, B, and C is useful for the purpose of this experiment, but raises a question about their origin. They must have been generated sometime in the 100s interval between launch and the start of picture taking. Three possible explanations are as follows: (a) the bubbles were released by the solid while being melted back by the spinning liquid and subsequently dispersed by fluid flow; (b) the bubbles were nucleated spontaneously due to the reduction of hydrostatic head upon attainment of low-gravity; or (c) the bubbles were nucleated by a particular vibrational frequency of the rocket motor. It is thought that (a) is unlikely since there were an extremely large number of bubbles, they were uniformly distributed throughout the liquid, and they were not situated on the tube wall as might be expected if they were dispersed by despin. It is not possible to distinguish between (b) and (c).

The existence of these small bubbles and their subsequent growth shows that they were in equilibrium with the liquid. In ground base experiments the opposite situation was observed, i.e., some bubbles released by the growing solid were seen to dissolve in the liquid during their rise to the top. The low-gravity behavior may have occurred because of the cooling of an initially saturated liquid or it may be a gravity related effect. Larson (Ref. 28) has shown that the reduction in hydrostatic head which occurs under gravity-free conditions can be accounted for by considering a reduced pressure regime in the P-T-X equilibrium diagram. When this is done, a liquid + gas two-phase equilibrium region can be encountered. Thus, a single phase liquid can, upon reduction of the applied pressure or hydrostatic head, transform to a liquid and gas mixture. Reduction in the hydrostatic head in order to allow gas phase formation is common practice in degassing of molten metals (Ref. 10). Variations in the total internal pressure from ampoule to ampoule and variations in the temperature in different locations in the liquid could then give rise to the observed variations in bubble densities. Bubbles never nucleated in the liquid during one-gravity simulation tests.

Growth of the bubbles during low-gravity occurred with a linear dependence of the radius on time (Fig. 4). If the growth had been controlled by diffusion through the liquid, a $t^{\frac{1}{2}}$ dependence should have been observed; however, a linear growth law is to be expected in the case of interfacial control of mass transport (Ref. 29). Interfacial control of the movement of dissolved gases into bubbles is often observed in steelmaking when surface active impurities are present (Ref. 30). The situation during the rocket experiment is complicated by the continuous cooling of the melt which changes the supersaturation thereby altering the growth kinetics.

The absence of any uniform, thermally driven bubble motion in the liquid portion of our specimens is consistent with the initial observations made on SPAR I. We are not able to ascribe this immobility to the lack of gravity because we think that a sufficient quantity of impurity was present to contaminate the bubble surface and arrest the flow. Earlier suppositions (Ref. 1) that the bubbles were immobilized by being in contact with the tube wall have been discounted because of the observation of nonuniform bubble motion in

specimen B. The bubbles were free to move. In addition, the flight film shows that the advancing interface obscured the bubbles. Therefore the bubbles were on the far side of the interface and couldn't have been against the nearer tube wall. In addition, the surfaces of the returned samples were smooth with no surface voids, i.e., all of the bubbles were totally enclosed by CBr_4. Other doubts about the absence of a temperature gradient in the liquid (Ref. 1) have been allayed by the spin table simulations mentioned above and in Ref. 27.

To investigate the effect of impurities on the thermal migration of bubbles, a series of simple laboratory tests were performed. These experiments are described more fully in Ref. 31, but mainly consisted of observing the effect of a temperature gradient on a bubble trapped in a horizontal tube. Pyrex sample tubes, 10 mm diameter by 100 mm long, were incompletely filled with various low-entropy of fusion organic materials. They were placed in the heat leveler block, turned to a horizontal position, melted, and brought to a stable, isothermal condition. The vapor bubble, 5-10 mm long by a 2-4 mm deep, which was present in the tube, was then brought to the center of the tube by mechanically leveling the heat leveler block (similar to the action of a carpenter's level). After static equilibrium was assured, the temperature of one end of the sample tube was raised by increasing power to one set of heaters, and the behavior of the bubble was monitored. In CBr_4 (melting point, T_m = 91°C, vapor pressure, P_m = 46 torr) the bubbles were generally immobile and their migration behavior was erratic and inconclusive. For commercial purity camphene (T_m = 51°C, P_m ≈ 20 torr), we observed consistent migration of the cold end at low values of $\Delta T/\Delta X$ (≈ 1°C/cm) and subsequent migration to the hot end when $\Delta T/\Delta X$ reached ≈ 3°C/cm. For partially purified camphene (5 pass zone refined), the bubbles were much less mobile than the CP material, but eventually moved to the hot end at high $\Delta T/\Delta X$. Bubbles in commercial purity succinonitrile (T_m = 58°C, P_m ≈ 0.1 torr) were generally immobile, but bubbles in succinonitrile of extremely high purity (supplied by M. Glicksman) were very mobile and consistently migrated to the hot end as soon as any temperature gradient was imposed. These ground base experiments were subject to the effects of buoyancy driven convection, and therefore the interpretation of observations of migration to the cold end of the tube is not unequivocal (see Ref. 31), but it is reasonable to conclude that impurities play a potent

role in determining the response of bubbles to thermal gradients and that the bubbles in our flight experiments with CP and ZR CBr_4 were subject to the influence of such impurities.

The observation of nonuniform bubble and fluid motion in sample B is puzzling. It seems clear that the downward motion of the large bubble caused displacement of fluid which in turn caused the smaller bubbles to move. The most likely driving force for the motion of the large bubble is surface tension, but the bubble moved from hot to cold. This is similar to some of the ground base observations mentioned above and is also reminiscent of observations of the motion of two phase inclusions in salt crystals, which also go from hot to cold (Ref. 32 and 33). The mechanism in that case was complex, involving evaporation and condensation. Alternatively, surface active impurities whose absorption is thermally activated can cause the temperature dependence of the surface tension to change sign (Refs. 34-36); this would result in a reversal of the predicted direction of motion. One of these mechanisms or modifications thereof might explain the motion of the large bubble. Alternatively, nonuniform wetting of the glass wall might have caused the motion. Bubble coalescence could not be the driving force because the observed motion was relatively uniform and low velocity, rather than abrupt and rapid. Likewise, shrinkage due to solidification and cooling could be expected to account for a maximum uniform downward motion of about (0.04) (6 mm) = 0.24 mm. The motion observed in sample B was much greater. Similarly, downward motion of the liquid is sometimes observed during directional solidification of plastic crystals; this is thought to be caused by aspiration of the melt into cracks and cavities which occur during cooling of the solid. This mechanism should, however, lead to a relatively uniform downward motion of liquid.

The forces imposed by nonuniform surface tension increase as the size of the bubble increases; therefore, larger bubbles should move before smaller ones. In view of our laboratory observations of erratic bubble migration behavior in CBr_4, it is perhaps not surprising that we saw bubble migration in only one of the four samples and that the bubble moved in the "wrong" direction. In retrospect, however, a sample material in which bubbles show a consistent and predictable response to thermal gradients would have been more satisfactory.

Subsequent to these observations, the film of SPAR I was reviewed at high speed. It was noticed that the abrupt coalescence of two large bubbles at the interface of one specimen caused a smaller bubble in the liquid to move a short distance (approximately 0.2 mm). Thus, we have another event in which the motion of a large bubble caused fluid flow and hence pushed neighboring small bubbles -- although the driving force in this instance was obviously coalescence. These observations document a source of fluid flow in low-gravity; namely, fluid motion due to bubble coalescence or due to the motion of large bubbles.

Since bubbles did not migrate through the liquid phase, it is unlikely that they would have been pulled off the solid-liquid interface by the thermal gradient. A calculation was made of the conditions under which thermocapillary forces would have been sufficiently strong to cause departure (Ref. 37). The results of this calculation show that, for the conditions present on SPAR III, the bubble diameter would have had to exceed 40 mm for departure in low-g as compared to 0.5 mm for departure in one-g. Alternatively, increasing the temperature gradient to 100°C/cm would have caused departure of a 2 mm bubble in low-g. These calculations did not take into account any impurity effects. These results indicate that thermal gradients may be of limited utility in low-gravity bubble management schemes.

SUMMARY

1. Specimens of nitrogen-saturated CBr_4 contained a larger total volume of trapped gas bubbles when solidified in a low-gravity environment. This is attributed to the absence of buoyancy forces.

2. In general, a larger number of trapped bubbles were present in the low-gravity specimens. This is indicative of easier bubble nucleation in low-gravity.

3. The morphology of grown-in voids (trapped bubbles) was found to be dependent upon the applied temperature gradient. A temperature gradient of 20°C/cm resulted in cylindircal voids, whereas a gradient of 5°C/cm resulted in spherical voids, all other things being equal.

The void morphology was dependent on gravity in the case of zone refined material only.

4. An initial temperature gradient of 20°C/cm did not cause bubbles to detach from a liquid-solid interface or to migrate to the hot end in liquid CBr_4 in low-gravity. Variable or inconsistant bubble migration behavior is to be expected for impure materials.

5. Solidification interfaces in CBr_4 were not able to cause long distance (greater than 1.0 mm) pushing of bubbles in low-gravity.

6. Motion or coalescence of bubbles can cause significant fluid flow in weightless liquids.

REFERENCES

1. Papazian, J.M. and Wilcox, W.R.: The Interaction of Bubbles with Solidification Interfaces. AIAA J., vol. 16, May 1978, pp. 447-451.

2. Haggard, J.B., Jr.: and Masica, W.J., Jr.: Motion of Single Bubbles Under Low Gravity Gravitational Conditions. Lewis Research Center, NASA TN D-5462, 1969.

3. Wilcox, W.R.; and Kuo, V.H.S.: Gas Bubble Nucleation During Crystallization. J. Crystal Growth, vol. 19, 1973, pp. 221-228.

4. Yee, J.F.; Sen, S.; Smara, K.; Lin, Mu-C.; and Wilcox, W.R.: Directional Solidification of InSb-GaSb Alloys. Proceedings of the Third Space Processing Symposium, Marshall Space Flight Center, Huntsville, Alabama M-74-5, June 1974, p. 301.

5. Larson, D.J.: Skylab M553 Sphere Forming Experiment. Proceedings of the Third Space Processing Symposium, p.101.

6. Deruyttere, A.; Aernoudt, E.; Gueminne, M.; Smeesters, J.; Arkens, O.; and Verhaeghen, M.: M565 Silver Grids Melted in Space. Proceedings of the Third Space Processing Symposium, p. 159.

7. Kawada, T.; Takahashi, S.; Yoshida, S.; Ozaqa, E.; and Yoda, R.: Preparation of a Silicon Carbide Whisker Reinforced Silver Composite Material in a Weightless Environment. Proceedings of the Third Space Processing Symposium, p. 203.

8. Uhlmann, D.R.: Massachusettes Institute of Technology, private communication, 1976.

9. Chalmers, B.: Principles of Solidification. John Wiley and Sons, Inc., New York, 1964, chapter 6.

10. Flemings, M.C.: Solidification Processing. McGraw-Hill, New York, 1974, chapter 6.

11. Piwonka, T.S.; and Flemings, M.C.: Pore Formation in Solidification. Trans. TMS-AIME, vol. 236, 1966, p. 1157.

12. Rocquet, P.; Rossi, J.C.; and Gironne, J. Adam.: Comparative Quality on Flat Rolled Products Produced from Continuously Cast and Conventionally Rolled Slabs. J. Metals, August 1967, pp. 57-61; and Recherches sur l'Effervescence lors de la Solidification de l'Acier. Revue de Metallurgie, vol. 4, April 1968, p. 257.

13. Burns, D.; and Beech, J.: Blowhole Formation During Solidification of Iron Alloys. Ironmaking and Steelmaking (Quarterly), 1974, no. 4, p. 239.

14. Vasconcellos, K.F.; and Beech, J.: The Development of Blowholes in the Ice/Water/Carbon Dioxide System. J. Crystal Growth, vol. 28, 1975, pp. 85-92.

15. Hills, A.W.D.; and Wells, I.C.: An Experimental Study of Bubble Nucleation During Solidification. Kinetics of Metallurgical Processes in Steelmaking. Dahl, W.; Lange, K.W.; and Papamantellos, D.; eds., 1975, p. 417.

16. Fredriksson, H.; and Svensson, I.: On the Mechanism of Pore Formation in Metals. Met. Trans., vol. 7B, p. 599, December 1976.

17. Shimura, F.; and Fujino, Y.: Crystal Growth and Fundamental Properties of $LiNb_{1-x}Ta_xO_3$. J. of Crystal Growth, vol. 38, no. 3, June 1977, pp. 293-302.

18. Carruthers, J.R.; and Nassau, K.: Nonmixing Cells Due to Crucible Rotation During Czochralski Crystal Growth. J. Appl. Phys., vol. 39, no. 11, October 1968, p. 5205.

19. Surface Tension in Fluid Mechanics. Educational Film no. 21610, Encyclopedia Britannica Educational Corporation.

20. Young, N.O.; Goldstein, J.S.; and Block, M.J.: The Motion of Bubbles in a Vertical Temperature Gradient. J. Fluid Mech., vol. 6, p. 350, 1959.

21. Coriell, S.R.; Hardy, S.C.; and Cordes, M.R.: Melt Shape in Weightless Crystal Growth. NBS Space Processing Research, NBSIR 77-1208, Annual Report, Feb. 1977, p. 72.

22. Grodzka, P.G.; Bourgeois, S.V.; Brashears, S.; and Spradley, L.W.: Fluid Motions in a Low-G Environment. Proceedings of the Third Space Processing Symposium, Marshall Space Flight Center, Huntsville, Alabama, M-74-5, June 1974, p. 691.

23. Ostrach, S.; and Pradham, A.: Surface Tension Induced Convection at Reduced Gravity. AIAA Paper No. 77-118, New York 1977.

24. Jackson, K.A.; and Hunt, J.D.: Transparent Compounds That Freeze Like Metals. Acta Met., vol. 13, 1965, p. 1212.

25. Gutowski, R.M.: Purification of Carbon Tetrabromide. M.S. Thesis, Clarkson College of Technology, 1977.

26. Papazian, J.M.; and Wilcox, W.R.: Flight III Technical Report for Experiment 74-36. Grumman Aerospace Corporation Research Department Memorandum RM-638, July 1977.

27. Mazzei, W.; Bondurant, R.A.; and Papazian, J.M.: Effect of Axial Spin and Despin on the Vertical Temperature Gradient in a Liquid Column. Grumman Aerospace Corporation Research Department Note RN-388, November 1977.

28. Larson, D., Jr.: Effects of Gravity Reduction on Phase Equilibria. Grumman Aerospace Corporation, Research Department Memorandum RM-608, September 1975, and RM-622, July 1976.

29. Christian, J.W.: The Theory of Transformations in Metals and Alloys, Part I, 2nd Ed., Pergamom Press, Oxford, 1975, Chapter 11.

30. Papamantellos, D.; Lange, K.W.; Okohira, K.; and Schenck, H.: A Mathematical Approach for the Mass Transfer Between Steel and an Ascending Bubble. Met. Trans., vol. 2, Nov. 1971, p. 3135.

31. Papazian, J., and Wilcox, W.R.: The Effect of Impurities on the Thermal Migration of Bubbles. To be published.

32. Wilcox, W.R.: Anomalous Gas-Liquid Inclusion Movement. Industrial and Engineering Chemistry, vol. 61, March 1969, pp. 76-77.

33. Anthony, T.P.; and Cline, M.E.: The Thermomigration of Biphase Vapor-Liquid Droplets in Solids. Acta Met., vol. 20, 1972, p. 247.

34. Jones, H.; and Leak, G.M.: The Effect of Surface Adsorbtion on Zero Creep Measurements in Iron-Silicon Alloys. Acta Met., vol. 14, 1966, p. 21.

35. Jones, H.; and Leak, G.M.: The Surface Entropy of Solid Metals. Metal Science Journal, vol. 1, 1967, p. 211.

36. Murr, L.E.: Interfacial Phenomena in Metals and Alloys. Addison-Wesley, Reading, Mass., 1975.

37. Cole, R.: Bubble Departure Radii at Solidification Interfaces. Chemical Engineering Department, Clarkson College of Technology, Potsdam, New York, 13676, to be published.

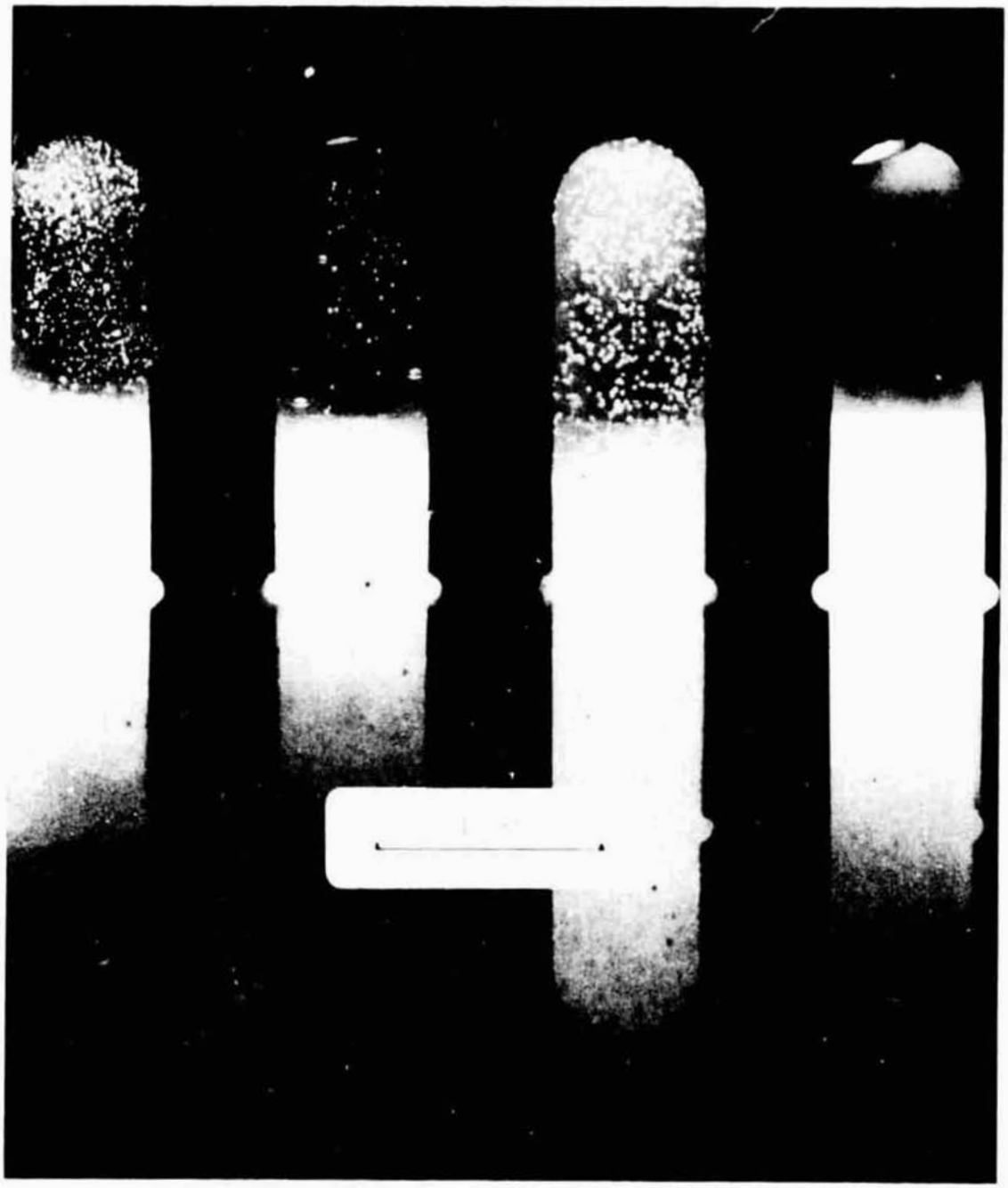

Fig. 1 Appearance of the specimens at 101s after lift-off. The specimens are designated A through D from left to right. The lower, bright portions are solid and the upper, dark portions are liquid. Fiducial grooves in the heat leveler block are spaced 10 mm center to center.

ORIGINAL PAGE IS
OF POOR QUALITY

ORIGINAL PAGE IS
OF POOR QUALITY

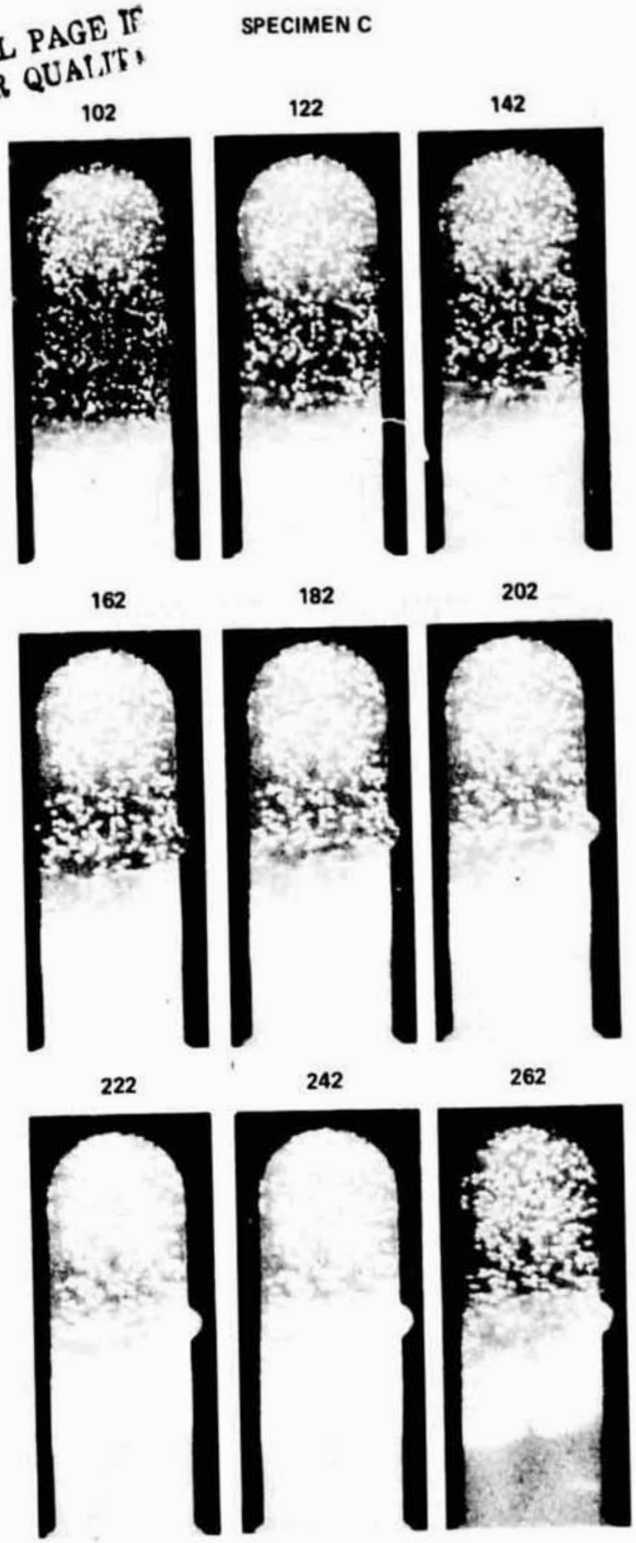

Fig. 2 Montage photograph of the growth of specimen B during SPAR III. The time from lift-off is shown above each view.

SPECIMEN B

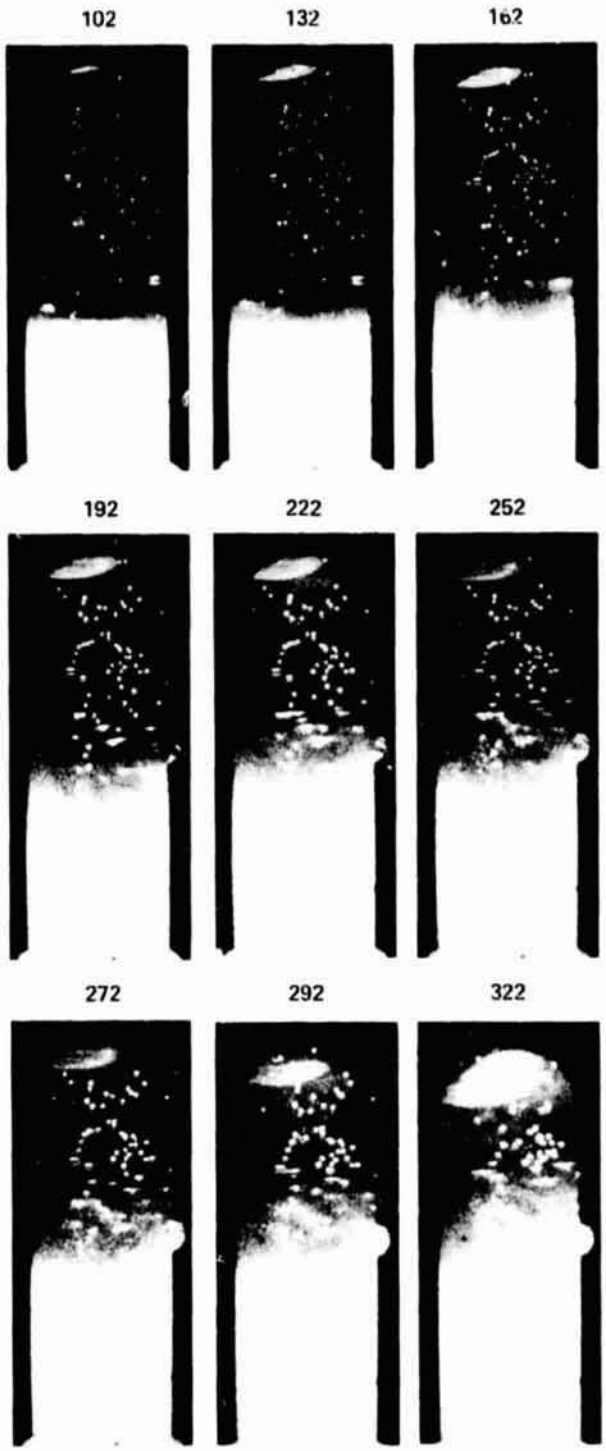

Fig 3 Montage photograph of the growth of specimen C during SPAR III. Same conditions as Fig. 2

ORIGINAL PAGE IS
OF POOR QUALITY

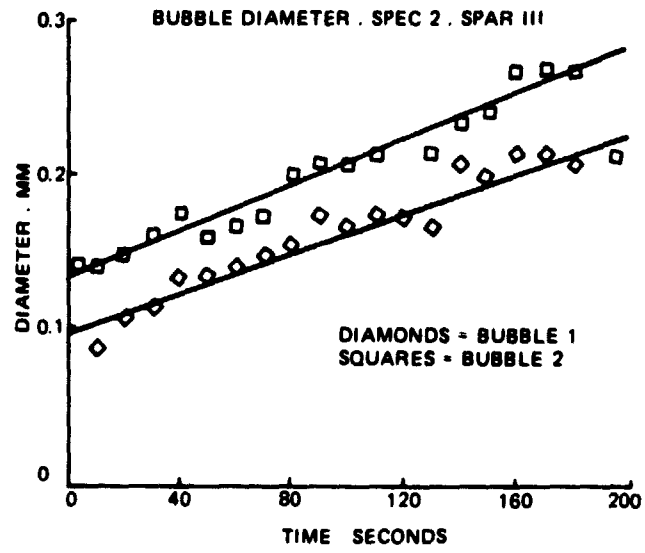

Fig. 4 Bubble diameters as a function of time, specimen B, SPAR III.